GRAIN SIZE AND STRUCTURE ANALYSIS OF POLYCRYSTALLINE SILICON ON GLASS FORMED BY ALUMINIUM-INDUCED CRYSTALLISATION FOR THIN-FILM SOLAR CELLS

Oliver Nast[a)*], Tom Puzzer[a)], Cheng Tsien Chou [b)], Mario Birkholz [c)]
[a)]Photovoltaics Special Research Centre, University of New South Wales, Sydney 2052, Australia
[b)] Pacific Solar, 82-86 Botany Street, Botany, NSW 2019, Australia
[c)] Hahn-Meitner-Institut, Abteilung Si-Photovoltaik, Kekuléstr. 5, D-12489 Berlin, Germany

ABSTRACT: One of the most challenging tasks in processing thin-film solar cells is the formation of high-quality polycrystalline silicon (poly-Si) on foreign substrates. Successfully achieving this, at low temperatures in short periods of time using industrially relevant techniques, promises to deliver a large reduction of solar cell fabrication costs. In this study, poly-Si films on glass that are formed employing an aluminium-induced layer exchange process are investigated. The process is based on isothermal annealing of thermally evaporated Al and sputtered a-Si layer structures at temperatures between 350°C and 525°C. A continuous poly-Si film can be formed in less than one hour. Various microscopy investigations in conjunction with x-ray diffraction measurements reveal that the grains of the poly-Si material are of preferential (100) orientation and some exceed 10 µm in size. The Al concentration in the crystallised films is analysed by comparing secondary ion mass spectroscopy results with Hall-effect measurement from earlier studies. The viability of the poly-Si films formed by the Al-induced layer exchange for thin-film solar cells is discussed.

Keywords: Silicon – 1: Recrystallisation – 2: thin-film - 3

1. INTRODUCTION

Silicon thin-film solar cells are seen as a promising technique to process cheap and efficient photovoltaic devices [1]. One of the challenges within the process is to achieve large-grained polycrystalline silicon (poly-Si) on foreign substrates at low temperatures in a reasonably short period of time. Large grain sizes of many microns seem mandatory to reach efficiencies in the range of 15 %. When the challenge can be met successfully, using industrially relevant techniques, a large reduction of solar cell fabrication costs is expected. As yet, no true low-temperature process for large-grained poly-Si (diameter of several µm) has emerged. One approach is the deposition of amorphous silicon (a-Si) on glass substrates with subsequent crystallisation. The two techniques, which have attracted most attention in this field, are (i) solid phase crystallisation (SPC) [2,3] and (ii) laser crystallisation (LC) [4,5]. SPC is an isothermal annealing process at temperatures above 600°C for an extended period of time (~50 hrs). The temperatures are still too high for low-cost substrates and time needed to achieve full crystallisation seems to be too long for an industrially relevant process. On the other hand the much faster laser crystallisation method suffers from possible contamination of the molten Si phase from low-temperature substrates. Additionally, this method can be regarded as an expensive technique compared to simple furnace annealing processes.

An alternative process to LC and SPC of a-Si is metal-induced crystallisation. It is well known that certain metals in contact with a-Si mediate the transformation process from the amorphous to the crystalline Si phase. This transformation occurs well below the eutectic temperature of the metal/Si system. Aluminium-induced crystallisation (AIC) is employed to epitaxially grow Si onto Si wafers in a process called solid phase epitaxy (SPE). During SPE a layered Si wafer/Al/a-Si structure is isothermally annealed at temperatures below the eutectic temperature of 577°C. The initial step of SPE is the dissolution of a-Si in Al, followed by the diffusion of the Si solute through the metal. Finally the Si grows epitaxially on the crystalline substrate [6]. Tsaur et al. successfully used SPE to form a Si solar cell by growing an epitaxial p-type emitter, due to Al doping, on top of an n-type wafer [7]. They achieved an open circuit voltage of 540 mV and an efficiency of 10.4%. Koschier et al. suggested the use of SPE for the formation of back-surface field layers on p-type substrates [8], and Wenham et al. used SPE, which they renamed to metal-mediated epitaxial growth, to investigate thyristor photovoltaic devices [9].

Based on SPE, aluminium-induced crystallisation can be applied for the formation of poly-Si films on glass. We recently showed that an Al/Si layer exchange process during the AIC process can lead to the formation of continuous poly-Si films at temperatures well below the eutectic temperature [10,11]. Figure 1 shows the overall layer exchange process as investigated in Ref.[12]. Since the processing temperatures are below 550°C, AIC can be considered as a true low-temperature process suitable for low-cost foreign substrates. Additionally, the aluminium-induced layer exchange process can be conducted in less than one hour. Due to the advantages of low-temperature and short-time processing, it is worthwhile analysing the material properties of the poly-Si layer with respect to its potential use for subsequent thin-film solar cell fabrication.

The study presented combines various microscopy techniques, x-ray diffraction, and secondary ion mass spectroscopy to investigate the poly-Si films formed during the Al-induced layer exchange process. The material parameters characterised are grain size, grain orientation, grain boundaries and Al concentration in the poly-Si film. All these parameters are important for the viability of the material in photovoltaic devices, since grain boundaries and crystallographic defects within the grains cause

* present address: Hahn-Meitner-Institut, Kekuléstr. 5, D-12489 Berlin, Germany,
phone: +49-30-67053305, fax: +49-30-67053-333, email: nast@hmi.de

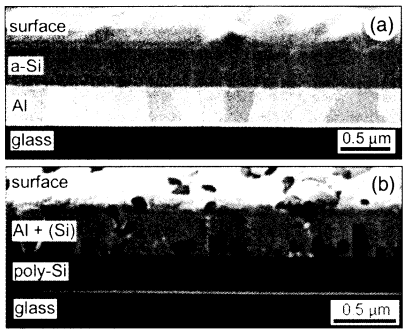

Figure 1: Cross section focused ion beam micrographs of a sample (a) before annealing and (b) after annealing for 60 min at 500°C; the samples are tilted by 45°.

recombination of electron-hole pairs and therefore limit the achievable conversion efficiency. Additionally, if the material is considered to serve as seeding layers for subsequent epitaxial growth, large grains of good crystallographic quality are required. The aim of the present paper is therefore to provide a comprehensive picture of the crystallographic nature of poly-Si material that is formed during the aluminium-induced layer exchange process.

2. EXPERIMENTAL DETAILS

The Al and a-Si layers were deposited onto glass (Corning 1737F) using thermal evaporation and dc magnetron sputtering, respectively. Prior to the Al evaporation the chamber was pumped down to $7x10^{-4}$ Pa. The following deposition was conducted at rates ranging from 0.5 to 10 nm/s. The amorphous silicon was deposited at a rate of 25 nm/min in a 1.5 Pa argon atmosphere at 100 W after the base pressure read below $2.4x10^{-4}$ Pa. A 100 mm, 120 Ωcm boron doped Czochralski-Si wafer was used as the sputtering target. No substrate heating was employed in either thermal evaporation or sputtering deposition. It has to be noted that the samples were exposed to air during the transfer from one deposition chamber to the other.

The isothermal annealing process of the Al and a-Si layer structure was conducted at temperatures ranging from 350°C to 525°C for annealing times from 5 min to 60 hrs. The heat treatment was performed in a furnace with dry N_2 ambient. It was interrupted by removing the samples from the furnace and cooling them to below 100°C in less than 2 min in a strong N_2 flow.

To investigate the bare poly-Si layer formed during annealing, the Al that had precipitated on the surface during the process was selectively etched off by a standard Al etching solution (80 parts phosphoric acid, 5 parts nitric acid, 5 parts acetic acid, and 10 parts deionized water at 50 to 55 °C). For various measurements the poly-Si film was lifted off the glass substrate, using concentrated HF, and transferred up-side down onto a tungsten substrate. This procedure allowed to investigate the clean, smooth former glass/film interface. Cracks, which developed in the film during the transfer process, were difficult to avoid.

The present study uses Scanning Electron Microscopy {(SEM), Hitachi S4500}, Transmission Electron Microscopy {(TEM), Philips CM200} and Orientation Imaging Microscopy {(OIM), TexSEM} to investigate the inner grain structure as well as grain sizes and the nature of the grain boundaries in the poly-Si films formed by AIC. The OIM captures and analyses the backscattered Kikuchi diffraction pattern (BKD) (also known as electron backscattering patterns) [13]. The BKD reveals the varying lattice orientation in the microstructure and, thus, allows to determine grain boundaries (GBs) due to the difference of lattice orientation from one side to the other. The OIM furthermore enables the classification of the grain boundaries and therefore allows a prediction for the electrical activity of these boundaries. In all OIM measurements the OIM boundary levels were set to 5°. The orientation of the grains was analysed using OIM as well as x-ray diffraction measurements (XRD). X-ray diffractograms of the poly-Si films were measured in symmetric θ–2θ geometry with CuKα radiation. Diffractograms of the four Si reflections of the poly-Si samples within $25° < 2\theta < 85°$ were recorded with a position sensitive detector, having Miller indices (111), (220), (311) and (400). The recorded Bragg reflections could well be fitted by appropriate line shape functions like splitted Lorentzians from which the integrated intensities were derived. Intensity values were corrected for finite absorption with a thickness-dependent absorption factor $A = (1-\exp(-2\mu d/\sin\theta))$ [14], where d accounts for the film thickness and $\mu = 148cm^{-1}$ denotes the X-ray absorption coefficient for Si and CuKα radiation.

The Al concentration is determined from secondary ion mass spectroscopy (SIMS) and compared to earlier Hall-effect measurements.

3. RESULTS AND DISCUSSION

3.1 Grain size and orientation

Recently it was shown that the Al-induced layer exchange process of Al/Si film structures appears to be driven by the dissolution of the a-Si into the Al through the Al/Si interface oxide [15]. The Si atoms, dissolved in the Al, diffuse and nucleate within the metal [11]. The growing grains replace the Al layer and finally form a continuous poly-Si film when complete coalescence occurs. Nast and Wenham used in-situ optical microscopy studies to determine the grain growth process [12]. Their investigations indicated that the formation of new nuclei ceases at an early stage of the crystallisation process, whilst the total number of grains is saturating, although only a minor fraction of the poly-Si film has formed. This effect was interpreted as an interference of neighbouring grains before actual coalescence occurs. The interference leads to the suppression of further nuclei formation. Extracting the saturated total number of grains in an analysed area, the average grain size could be calculated to be about 15 µm for a sample annealed at 450°C. This indirect grain size analysis is compared with direct grain size characterisation techniques in the following section.

A common technique to investigate grain size as well as crystallographic grain quality of poly-Si is the use of an etching solution that preferentially etches grain boundaries and defects. Figure 2 depicts a poly-Si film formed at 475°C where these grain boundaries and crystallographic faults are visualised due to chemical etching in a HNO_3/HF solution (100:1) for 30 sec. It is apparent from the figure

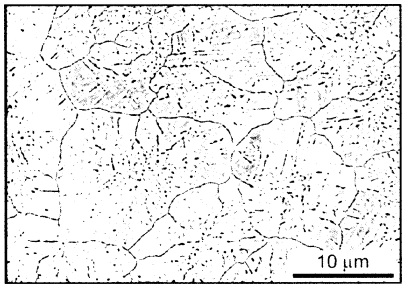

Figure 2: SEM image of poly-Si film after HNO_3/HF etching.

that some grains exceed 10 µm in size. However, the micrograph also reveals that grains appear to contain a subgrain-structure and numerous defects. The investigation of this substructure is important when the feasibility of the poly-Si material for subsequent device fabrication is studied. Already minor fractions of areas of lower crystallographic quality have a negative impact on the overall solar cell performance [16].

The difficulty arising from an etching step to analyse the crystallographic structure of poly-Si is that grain boundaries (GBs) and inner-grain faults are accentuated in the same way. The distinction between them is therefore complicated. In this case an orientation imaging microscope can serve as a powerful tool to investigate grain sizes and boundaries. Orientation imaging micrographs are the result of step-by-step analysis of the BKD with a step size of 0.36 µm in the following OIM study. Figure 3 shows an orientation imaging micrograph of a poly-Si film formed at 450°C. To avoid that rough surface features on top of the Si layer disturb the analysis, the film was etched of the glass substrate and transferred up-side down onto a metal substrate. This enabled the investigation of the smooth glass/poly-Si interface. The grey variation in the image is determined by the image quality factor (IQ). The IQ represents the contrast of the Kikuchi bands in the BKD pattern at each point. The dark area in the top half to the very right of the image is, for example, a crack in the Si film that occurred during the lift-off and transfer procedure. In this defect area no BKD with analysable contrast is detected. Consequently the IQ is low and the crack appears dark. The white and black lines in Figure 3 are boundaries between regions of different crystallographic orientations as extracted from the BKDs. As apparent from the micrograph, the poly-Si material consists of grains with sizes exceeding 10 µm, but there are also areas where the grain sizes are considerably smaller. The average grain size of the particular area analysed in Figure 3 is therefore reduced to 6.2 µm.

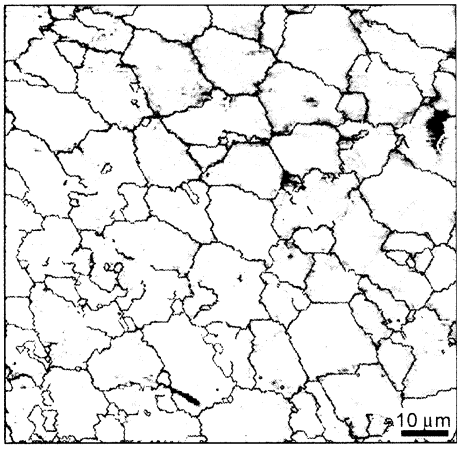

Figure 3: Orientation imaging micrograph depicting the grain sizes and grain boundaries. The white lines represent Σ3 and Σ9 CSL GBs, the black once all other types of GBs.

The existence of small grains seems to contradict the results presented on the in-situ optical microscopy studies mentioned above. According to that investigation, growing Si grains interfere at an early stage of the crystallisation process and suppress the formation of new nuclei. Therefore, if large grains are formed small grains should be very rare. In this case *large* and *small* means above 10 µm and below 5 µm in diameter, respectively.

The grain boundaries of the poly-Si material analysed in Figure 3 can be separated into two groups: (a) coincident site lattice grain boundaries, CSL GBs, with coincidence index Σ3 and Σ9 (white lines) and (b) all other types of GBs (black lines). The ratio of Σ3 to Σ9 GBs amongst the white lines is about unity. It is apparent from the micrograph that the grains in the small-grained areas are predominantly separated by Σ3 and Σ9 grain boundaries. Both types of CSL GBs have low atomic distortions [17]. Fedotov et al. showed that Σ3 and Σ9 GBs in silicon are electrically inactive grain boundaries in as grown crystals [18]. However, in the discussion of orientation imaging microscopy studies it has to be mentioned that the grain boundary classification is determined by the orientation of neighbouring crystal areas and that the actual structure of the grain boundary remains unknown. It is an assumption that the grain boundary plane itself resembles the theoretical CSL GB structure.

We also conducted OIM measurements on large isolated grains. The analysis revealed that these grains, although grown from individual nuclei, contain Σ3 and Σ9 GBs. We therefore conclude that these types of GBs develop during the grain growth process. The occurrence of Σ3 and Σ9 twin boundaries in as-grown grains can be attributed to the dendritic growth behaviour during metal-induced crystallisation [19].

The apparent contradiction of the optical microscopy and the OIM studies concerning the grain size and small-grained areas can therefore be resolved as follows. In the optical microscope analysis a grain is classified as a crystalline Si area grown from one nucleus. Crystallographic faults like the development of a twin grain boundary is not observable. This is different in OIM investigations where a grain is detected as an area of identical crystallographic orientation. From the combination of the results of both methods the polycrystalline Si layer can be seen as large-grained material with some grains containing a subgrain structure. This structure consists of areas of different crystallographic orientations separated by CSL grain boundaries with indices Σ3 and Σ9.

Besides the grain boundary analysis, the OIM reveals the crystallographic orientation of the Si crystals extracted from the BKD pattern. Figure 4 shows two OIM images taken from samples that had been annealed at 450°C and 525°C. Figure 4a is the same measurement as Figure 3, but this time the grain orientations are displayed instead of the

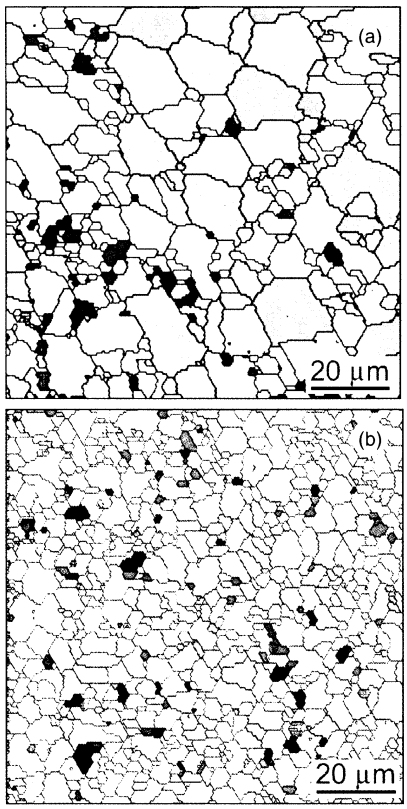

Figure 4: Orientation imaging micrographs of samples annealed at (a) 450°C and (b) 525°C. The black lines represent grain boundaries. The dark grey areas are grains with (111) orientation except of 9 grains in (a) and 16 grains in (b) with (110) orientation. All light grey areas are orientated in the (100) direction.

IQ. The dark grey areas represent (111) and (110) orientation combined, while the light grey shading stands for grains orientated in the (100) direction. All other grains (white) are orientated in neither of these three directions. Amongst the dark grey grains there are only a small fraction orientated in the (110) direction (9 and 16 grains in (a) and (b), respectively). The images reveal two aspects of special interest: (i) the grains are larger when the poly-Si film is formed at lower temperatures and (ii) there seems to be a preferential (100) orientation especially of the larger grains. The (100) orientation is prevalent in the middle area of the upper half of the image shown in Figure 4a containing large grains (>15 µm).

The finding of the OIM investigation that the grain sizes increase with decreasing annealing temperature clearly supports results presented in earlier studies based on optical microscopy and SEM investigations [12]. The preferential (100) orientation, as extracted from OIM measurements analysing an area of 100x100 µm^2, is verified by XRD measurements. The analysed spectra shown in Figure 5 are taken from a sample area of many mm^2.

In Figure 5 the four reflections of a 250 nm thick sample are displayed that have been corrected by dividing the measured intensities with the thickness-dependent absorption factor A. The intensities are normalised with respect to the (111) Bragg reflection, which is set to 100 %. The figure also displays the integral intensities of a silicon powder according to JCPDS card 27-1402 [20] with a

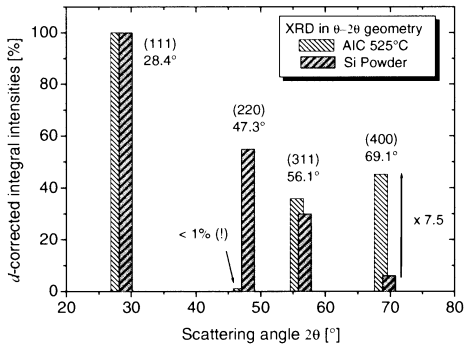

Figure 5: XRD measurements presenting the integral intensities of poly-Si film formed at 525°C (AIC 525°C) compared to a standard Si powder. The film thickness d has been taken into consideration.

random orientation of grains. Two interesting facts can be seen from the comparison of both intensity sets. Firstly, the (220) reflection in the poly-Si film formed using AIC (AIC film) is found to be negligibly small in comparison to a random orientation. It can be concluded that the growth of silicon grains with (110) crystallographic lattice planes parallel to the substrate is insignificant in poly-Si films formed by the Al-induced layer exchange. Secondly, the (400) reflection is seen to be enhanced by a factor of 7.5 in comparison to a randomly orientated ensemble of Si grains. This effect of enhanced (100) orientation has also been observed for AIC films formed at other temperatures (425°C, 450°C and 475°C) and corroborates the result of the OIM investigation. It can be concluded that AIC films exhibit a (100) texturing that contrasts to poly-Si processed by SPC or LC, which is of preferred (111) orientation [21,22]. This effect qualifies AIC films as seeding layers for epitaxial thin-film silicon growth, since successful epitaxial growth was observed by many investigators to occur preferentially on (100) orientated Si substrates [23]. For potential use as seeding layers more convenient layer sequences such as poly-Si/back contact/substrate structures can easily be formed employing the Al-induced layer exchange process [24].

3.2 Inner grain structure

Information on the inner grain structure of the poly-Si was provided by TEM investigations. Two images are shown in Figure 6 taken from a sample annealed at 450°C. Both images exhibit black areas that are a couple of 100 nm in size. These areas are holes in the thinned TEM specimens. They originate from Al clusters that had been trapped between the continuous poly-Si film and the glass substrate. The appearance of these Al clusters was recently investigated in Ref. [12].

Figure 6a reveals typical bend contours in the form of white wavy lines, which indicate the good quality of single-crystal material. Figure 6b taken at higher magnification shows the primary intragrain twin defects that can be found in the material. Comparing these images to TEM investigations on SPC poly-Si [25], it becomes apparent that the poly-Si material formed by an Al-induced layer exchange process is of superior crystallographic quality. We attribute this difference to the fact that during the layer exchange no atom remains where it was, but a complete

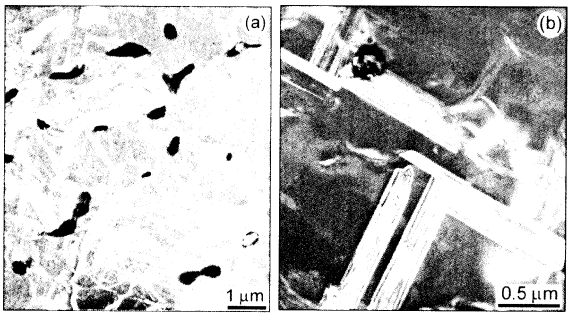

Figure 6: Bright-field TEM images taken from a sample annealed at 450°C at different location and magnification.

dissolution and restructuring process of the Si phase takes place. Additionally, it is worthwhile mentioning that we could not find any evidence of an enhanced Al concentration at grain boundaries according to electron dispersive x-ray spectroscopy.

3.3 Al concentration

One of the most important questions when studying poly-Si material formed using AIC is the amount of Al that is incorporated into the Si film. To elucidate the actual Al concentration within the poly-Si, a fully crystallised film, annealed at 500 °C, was lifted off the glass substrate, turned up-side down and transferred to a metal substrate. SIMS measurement were conducted on the 500 nm thick layer starting the depth profile at the smooth, clean surface of the former glass/poly-Si interface. For a quantitative analysis a c-Si wafer with 10^{20} cm^{-3} Al atoms ion-implanted served as a calibration standard. The measurement shown in Figure 7 reveals that the poly-Si layer predominantly contained Al at a concentration of about $3\text{x}10^{19}$ cm^{-3} (0.06 at%).

The SIMS depth profile shows two areas of increased Al concentration. The local maximum after a sputtering time of 500 s can be attributed to an Al-oxide layer at the former poly-Si/Al interface. This oxide layer is formed during the sample transfer from the thermal evaporator to the sputtering chamber when the original layer structure is deposited. Nast and Hartmann recently showed that this Al oxide layer is stable during the entire layer exchange process [15]. The fact that the Al concentration does not decrease abruptly at depths beyond the poly-Si/Al interface is due to residual Si crystals that were formerly embedded in the Al matrix and are connected to the continuous poly-Si layer. The second area of increased Al concentration is found at the former poly-Si/glass interface. The enhanced concentration of Al in form of Al oxide at the glass/poly-Si interface can be understood when the interaction of the Al film and the glass is considered. Before annealing the Al layer was in direct contact with the glass substrate. The Al reduces the SiO_2 of the glass and a thin stable aluminium oxide layer is formed during the annealing process, whilst the Al itself is replaced by the poly-Si film.

Since Al is a well-known acceptor in Si, it is no surprise that the poly-Si films are of p-type conductivity. The hole concentration is about $2.5\text{x}10^{18}$ cm^{-3} according to Hall-effect measurements [11]. Whilst the measured hole concentration is equal to the ionised Al atoms on substitutional sites, Al_{sub}^-, the SIMS results give the total

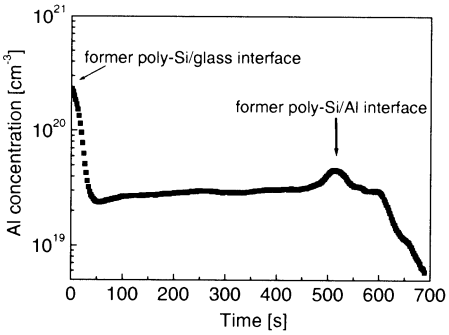

Figure 7: SIMS measurement of a poly-Si film turned up-side down. The Al concentration is graphed versus depth given as sputtering time.

amount of Al in the poly-Si material Al_{tot}. To compare the Hall-effect measurements with the SIMS result it is necessary to calculate the total concentration of Al atoms on substitutional sites, Al_{sub}. For the calculation, the Fermi energy can be extracted from

$$p = \frac{1}{2\pi^2}\left(\frac{2m_{dv}}{\hbar}\right)^{1.5}\int_{-\infty}^{0}\frac{\sqrt{-E}}{e^{(E_F-E)/kT}+1}dE \qquad (1)$$

with m_{dv} being the valence-band density-of-states effective mass, E_F the Fermi level, $\hbar$ the reduced Planck constant and k the Boltzmann constant. We assume a parabolic band structure of the valence band and set the valence band edge equal to zero. Due to the high doping concentration, the following analysis refrains from approximating the Fermi distribution by the Boltzmann distribution to avoid inconsistencies due to degeneration effects. Using the Fermi integral $F_{1/2}$ equation (1) can be written as

$$p = N_V \cdot F_{1/2}[-E_F/kT] \qquad (2)$$

with

$$N_V = 2\left(\frac{m_{dv}kT}{2\pi\hbar^2}\right)^{1.5}. \qquad (3)$$

Green gave for the effective density of states the value N_V equal to $3.10\text{x}10^{19}$ cm^{-3} using his reassessed value for the valence-band density-of-states effective mass at T = 300 K [26]. Knowing the free carrier concentration and using Fermi integral tables, equation (2) enables to extract the Fermi energy [27]: $E_F = 65 \pm 2$ meV. The error stems from variations in the determined hole concentration in Ref.[11].

The free carrier concentration equals the negatively ionised Al atoms on substitutional Si lattice site. (Counter-doping due to impurity incorporation such as oxygen is neglected, because of the high doping level.) The ratio x of ionised substitutional Al atoms to the total amount of substitutional Al atoms is determined by the following relationship [28]

$$x = \frac{Al_{sub}^-}{Al_{sub}} = \frac{1}{g \cdot e^{(E_A-E_F)/kT}+1} \qquad (4)$$

E_A is the activation energy and g is the ground-state degeneracy factor, which equals 4 for acceptor levels in Si. Using 54 meV as the activation energy E_A, the value determined in an earlier study [11], and a Fermi energy of 65 meV, the ratio x equals 0.28. Consequently, only about

28% of the Al atoms on substitutional sites are ionised and therefore contribute to the free carrier concentration of the poly-Si at room temperature. Using equation (4) the total amount of Al atoms on lattice sites can be determined: $Al_{sub} = (1.0\pm0.5)x10^{19}$ cm^{-3}. The upper limit of this value is related to calculations using an upper limit of the activation energy of Al in only lightly doped silicon, which is 67 meV [28]. The lower limit is determined by assuming compensation from incorporated oxygen. Furthermore, it is likely that an Al impurity band is formed in the energy band structure of the highly doped poly-Si material. It is unknown whether influences of this Al band can be entirely neglected even at room temperature. Nevertheless, the comparison of the total amount of Al as revealed by SIMS to the concentration of Al on substitutional sites as extract from Hall-effect measurements shows that both results are of the same order of magnitude.

Hole concentrations in the order of 10^{18}-10^{19} cm^{-3} limit the minority carrier lifetime in crystalline silicon to between 100 ns and 1 µs due to Auger recombination. If Auger recombination was also the dominant recombination factor in the large-grained poly-Si material formed by AIC, the p-type films could be used as absorber material in thin-film solar cells of a thickness of a couple of µm with advanced light trapping. Studies of the carrier life time and diffusion length in the poly-Si film formed by AIC are currently under investigation.

4. CONCLUSION

The Al-induced layer exchange process leads to the transformation of a-Si to poly-Si at low temperatures (<550°C) using industrially relevant techniques. The poly-Si material formed contains grains with sizes exceeding 10 µm. The grains are preferentially (100) orientated and their inner grain quality is superior to solid phase crystallised material. The Al concentration in the poly-Si films is in the order of 10^{19} cm^{-3}. Due to the simplicity of the process, the usage of industrially relevant techniques, short-time and low-temperature processing, the Al-induced layer exchange seems to be of great interest for subsequent thin-film solar cell fabrication.

ACKNOWLEDGEMENT

We would like to acknowledge the support of S. R. Wenham, M. A. Green, and other members of the Photovoltaics Special Research Centre, as well as W. Fuhs from the Hahn-Meinter-Institut Berlin. We thank S. Brehme (HMI) for the Hall-effect measurements. We further appreciated the opportunity for using the OIM at Pacific Solar. O. Nast acknowledges the support of the German Academic Exchange Service (DAAD) under the HSPIII program.

REFERENCES

[1] R. B. Bergmann, Applied Physics A **69**, 187 (1999).
[2] R. S. Sposili and J. S. Im, Appl. Phys. Lett. **69**, 2864 (1996).
[3] R. B. Bergmann, G. Oswald, M. Albrecht, and V. Gross, Solar Energy Materials and Solar Cells **46**, 147 (1997).
[4] T. Matsuyama, N. Terada, T. Baba, T. Sawada, S. Tsuge, K. Wakisaka, and S. Tsuda, J. Non-Crystall. Solids **198-200**, 940 (1996).
[5] K. Ishikawa, M. Ozawa, C.-H. Oh, and M. Matsumura, Jpn. J. Appl. Phys. **37**, 731 (1998).
[6] G. Ottaviani and G. Majni, J. Appl. Phys. **50**, 6865 (1979).
[7] B. Y. Tsaur, G. W. Turner, and J. C. C. Fan, Appl. Phys. Lett. **39**, 749 (1981).
[8] L. M. Koschier, S. R. Wenham, M. Gross, T. Puzzer, and A. B. Sproul, "Low Temperature junction and back surface field formation for photovoltaic devices," presented at the *2nd World Conference and Exhibition on Photovoltaic Solar Energy Conversion*, Vienna, Austria, 1999, p. 1593
[9] S. R. Wenham, L. M. Koschier, O. Nast, and C. B. Honsberg, IEEE Transactions on Electron Devices **46**, 2005 (1999).
[10] O. Nast, T. Puzzer, L. M. Koschier, A. B. Sproul, and S. R. Wenham, Appl. Phys. Lett. **73**, 3214 (1998).
[11] O. Nast, S. Brehme, D.-H. Neuhaus, and S. R. Wenham, IEEE Transactions on Electron Devices **46**, 2062 (1999).
[12] O. Nast and S. R. Wenham, J. Appl. Phys. in print
[13] B. L. Adams, S. I. Wright, and K. Kunze, Metallurgical Transactions A **24A**, 819 (1993).
[14] M. Birkholz, S. Fiechter, A. Hartmann, and H. Tributsch, Phys. Rev. B **43**, 11926 (1991).
[15] O. Nast and A. J. Hartmann, J. Appl. Phys., in print
[16] H. Nagel, A. G. Aberle, and S. Narayanan, Solid State Phenomena **67-68**, 503 (1999).
[17] A. V. Nikoaleva and Y. A. Nikoalev, Materials-Science-Forum **207-209**, 657 (1996).
[18] A. Fedotov, B. Evtodyi, L. Fionova, Y. Ilyashuk, E. Katz, and L. Polyak, Physica-Status-Solidi-A **119**, 523 (1990).
[19] S. R. Herd, P. Chaudhari, and M. H. Brodsky, J. Non-Crystall. Solids **7**, 309 (1972).
[20] NBS Standard Reference Material No. 640. Report No. Vol. 13, 1976.
[21] L. Haji, P. Joubert, J. Stoemenos, and N. A. Economou, J. Appl. Phys. **75**, 3944 (1994).
[22] S. Loreti, M. Vittori, L. Mariucci, and G. Fortunato, Solid State Phenomena **67-68**, 181 (1999).
[23] J. Platen, B. Selle, I. Sieber, U. Zimmer, and W. Fuhs, Mat. Res. Soc. Symp. Proc. **570**, 91 (1999).
[24] O. Nast, S. Brehme, S. Pritchard, A. G. Aberle, and S. R. Wenham, Solar Energy Materials and Solar Cells, in print
[25] T. Noma, T. Yonehara, and H. Kumomi, Appl. Phys. Lett. **59**, 653 (1991).
[26] M. A. Green, J. Appl. Phys. **67**, 2944 (1990).
[27] J. S. Blakemore, *Semiconductor Statistics*, Dover edition (General Publishing Company, Toronto, 1987).
[28] S. M. Sze, *Physics of Semiconductor Devices*, 2 ed. (Wiley & Sons, New York, 1981).